Journal of Power Sources 275 (2015) 189–199

Contents lists available at ScienceDirect

Journal of Power Sources

journal homepage: www.elsevier.com/locate/jpowsour

Palladium and palladium–tin supported on multi wall carbon nanotubes or carbon for alkaline direct ethanol fuel cell

Adriana Napoleão Geraldes [a], Dionisio Furtunato da Silva [b], Júlio César Martins da Silva [b], Osvaldo Antonio de Sá [a], Estevam Vitório Spinacé [b], Almir Oliveira Neto [b], Mauro Coelho dos Santos [a, *]

[a] Laboratório de Eletroquímica e Materiais Nanoestruturados, Centro de Ciências Naturais e Humanas, Universidade Federal do ABC, Rua Santa Adélia, 166, 09210-170 Santo André, SP, Brazil
[b] Instituto de Pesquisas Energéticas e Nucleares-Comissão Nacional de Energia Nuclear (IPEN-CNEN), Av. Prof. Lineu Prestes, 2242, 05508-900 São Paulo, SP, Brazil

HIGHLIGHTS

- The use of MWCNT, instead of C, improves the electrocatalytic activity for EOR.
- Addition of small amount of Sn to Pd improves the electrocatalytic activity for EOR.
- PdSn/MWCNT electrocatalyst showed increase performance for ethanol oxidation.
- Electrocatalysts supported on MWCNT show higher power densities.
- ATR-FTIR *in situ* identifies acetate and acetaldehyde as products formed during EOR.

ARTICLE INFO

Article history:
Received 2 September 2014
Received in revised form
19 October 2014
Accepted 5 November 2014
Available online 6 November 2014

Keywords:
Electron beam irradiation
Multi wall carbon nanotubes
Carbon
Alkaline direct ethanol fuel cell
Ethanol electro-oxidation

ABSTRACT

Pd and PdSn (Pd:Sn atomic ratios of 90:10), supported on Multi Wall Carbon Nanotubes (MWCNT) or Carbon (C), are prepared by an electron beam irradiation reduction method. The obtained materials are characterized by X-Ray diffraction (XRD), Energy dispersive X-ray analysis (EDX), Transmission electron Microscopy (TEM) and Cyclic Voltammetry (CV). The activity for ethanol electro-oxidation is tested in alkaline medium, at room temperature, using Cyclic Voltammetry and Chronoamperometry (CA) and in a single alkaline direct ethanol fuel cell (ADEFC), in the temperature range of 60–90 °C. CV analysis finds that Pd/MWCNT and PdSn/MWCNT presents onset potentials changing to negative values and high current values, compared to Pd/C and PdSn/C electrocatalysts. ATR-FTIR analysis, performed during the CV, identifies acetate and acetaldehyde as principal products formed during the ethanol electro-oxidation, with low conversion to CO_2. In single fuel cell tests, at 85 °C, using 2.0 mol L^{-1} ethanol in 2.0 mol L^{-1} KOH solutions, the electrocatalysts supported on MWCNT, also, show higher power densities, compared to the materials supported on carbon: PdSn/MWCNT, presents the best result (36 mW cm^{-2}). The results show that the use of MWCNT, instead of carbon, as support, plus the addition of small amounts of Sn to Pd, improves the electrocatalytic activity for Ethanol Oxidation Reaction (EOR).

© 2014 Elsevier B.V. All rights reserved.

1. Introduction

Environmental problems and the increased global demand for energy have mobilized the scientific community in search for clean and renewable energy sources [1–3]. Fuel cell (FC) systems represent a technological approach, which meets all requirements for a future sustainable conversion technology with high electrical efficiency, low emissions and the possibility of cogeneration (energy and heat). FC appears to be an appropriate technology for generating electricity through hydrogen or alcohol electro-oxidation: the acid fuel cells are the most developed variety of this procedure [4–8]. However, the slow electrode kinetics, the CO poisoning of noble metal based electrocatalysts, high costs of electrocatalysts

* Corresponding author.
E-mail addresses: drinager@ig.com.br (A.N. Geraldes), dfsilva@ipen.br (D. Furtunato da Silva), quimijulio@yahoo.com.br (J.C. Martins da Silva), osvaldosa@bol.com.br (O. Antonio de Sá), espinace@ipen.br (E.V. Spinacé), aoneto@ipen.br (A.O. Neto), pdrmcsa@gmail.com (M. Coelho dos Santos).

http://dx.doi.org/10.1016/j.jpowsour.2014.11.024
0378-7753/© 2014 Elsevier B.V. All rights reserved.

and proton exchange membranes, such as Nafion®, are some of challenges to be overcome [4–8].

The direct alcohol fuel cells (DAFCs) are acidic fuel cells that oxidize alcohols directly and have greater advantages compared to fuel cells fed with hydrogen, due to the fuel properties, such as: easy storage and handling, high energy density and wide availability. These characteristics make alcohols attractive liquid fuels in the majority of promising alternative power sources for transportation, portable electronics and stationary applications [7].

Methanol is the most utilized liquid fuel but ethanol, which is easily produced in a large quantity, via fermentation of biomass, is a green, sustainable and carbon–neutral type of fuel, with higher energy density and lower toxicity than those of methanol, so it has been widely studied due to its economic and environmental characteristics. However, the complete oxidation of ethanol to CO_2 is more difficult than methanol, due to the requirement of C–C bond breaking and the formation of CO-like species that poison the platinum-based electrocatalysts used in acidic fuel cells [9–11].

It is well known that Alkaline Direct Alcohol Fuel Cells (ADAFC) have numerous advantages over the acidic fuel cells (DAFC) owing to their favorable kinetic of anodic reactions of ethanol electro-oxidation in alkaline media, due to the weaker binding between the electrocatalyst and adsorbed intermediates such CO and CO-like species. In these cells, the kinetic of cathodic reactions is, also, favored because it require slower over-potentials for the reduction of oxygen to OH^-. Furthermore, in the single fuel cell, higher power densities can be obtained due to the reduced alcohol cross over from the anode compartment to the cathode compartment, by electro-osmotic drag, since in the exchange anionic membranes, the hydrate hydroxyl ions displacement occurs in the opposite direction of the alcohol displacement. This fact facilitates the water management in the cell, preventing both anode dryness and cathode flooding, once water is formed in both anodic and cathodic reactions and the water formed at the cathode would be dragged to anode accompanying hydrate hydroxyl ions [12].

The fastest kinetic of the alcohol oxidation reaction in alkaline direct alcohol fuel cell (ADAFCs) provides the possibility of using less expensive metal catalysts, such as palladium, tin, silver, and nickel that make the alkaline direct alcohol fuel cells a potentially low-cost technology, compared to acid direct alcohol fuel cells, which employ based-platinum electrocatalysts [7,12]. Palladium-based nanocatalysts have continued to receive many efforts in their development because of their cost advantage, relative abundance and unique properties in the alcohol electrocatalytic oxidation, in alkaline media, compared to platinum catalysts. Palladium is more abundant in nature and cheaper than platinum. Economic advantages of using the ADAFCs to using others than the Pt electrocatalysts are evident, when comparing the cost of Pt gram (€ 46), Au (€ 42.5), Pd (€ 19), Ni (€ 0.01) and Sn (€ 0.01): there is a significant reduction of research costs [7].

Another point to be considered for the development of fuel cell technology is the choice of support. The main requirements of a suitable support for a fuel cell electrocatalyst are high surface area, good electrical and thermal conductivity and suitable porosity to allow a good reactant flow and high stability in the FC environment. Carbon black (CB or C) presents most of these characteristics, however, in long-term experiments, it exhibits low stability to corrosion, especially in acidic media at high potentials (cathode side) and high temperatures (>90 °C). On the other hand, the large availability and the low cost make CBs and, in particular, Vulcan-type materials, still the most diffuse supports for low-temperature FC electrocatalysts. The high crystalline status of carbon nanotubes (CNTs) makes these materials highly conductive, while the high surface area and the great number of mesopores can lead to high metal dispersion and a good reactant flux in the tubular graphite structure. It has been established that the increase in the graphitization degree of the carbon material increases the π sites, which can act as anchoring centers for the metallic nanoparticles. As a result, the metal-support interactions and the resistance of the support to oxidation are improved [12].

Pt/C and PtSn/C were studied in our group [5,13–18] and PtSn/C electrocatalysts have been described as more active for ethanol electro-oxidation in acid medium [13]. Carbon-supported metal nanoparticles for fuel cell applications have been prepared by radiation-induced reduction of metal ion precursors [13]. Silva et al. studied the activities of different electrocatalysts for alcohol electro-oxidation in an alkaline medium and reported that PtAu/C electrocatalysts presented superior performance towards ethanol electro-oxidation than Pt/C electrocatalysts; moreover, PtAuBi/C (50:40:10) showed a better performance than PtAu/C, in alkaline conditions [16]. De Souza et al. [18] reported that Pt/C-Etek presented a different activity for the EOR, depending on the substrate. Pt/C on carbon cloth facilitated the C–C bond cleavage of the ethanol molecules, via a new ATR–FTIR setup introduced *in situ* spectra-electrochemical studies, in non-reflective and rough electrodes.

Jiang et al. [19], also, studied the Pt and PtSn carbon-supported prepared by modified polyol method. The electrocatalytic activities and stabilities of the Pt/C and PtSn/C catalysts towards ethanol electro-oxidation reactions (EORs) were investigated by potentiodynamic and potentiostatic methods, in alkaline and acid media. On both catalysts, the EOR currents in the alkaline solutions were much higher than those in acid solutions, and the onset potentials of the EOR, in alkaline solutions, were less positive than those in acid solutions, indicating that the kinetics of the EOR improves in alkaline solutions.

Pd-based catalysts have shown appreciable performance toward the EOR in alkaline media [12]. He Q. et al. [20] studied the activities of $Pd_{2.5}$ Sn/C and Pd_4Au/C electrocatalysts for ethanol electro-oxidation in alkaline medium by cyclic voltammeter, fast chronoamperometry and impedance spectroscopy. Pd_4Au/C displayed better catalytic activity than $Pd_{2.5}$ Sn/C and the commercial Pt/C (E-TEK Inc.). Modibedi et al. [21] studied PdSn/C and PdRuSn/C nanocatalysts prepared by the chemical reduction method, using sodium borohydride and ethylene glycol mixture, as the reducing agent. The current density obtained for the ethanol electro-oxidation was affected by varying ethanol concentration between 0.25 and 4 mol L^{-1}. Raising ethanol concentration up to 3.0 mol L^{-1} increased the coverage of the adsorbed ethoxy (CH_3CO_{ads}) species on the nanocatalyst surface, thus yielding an increase in current density. PdSn/C displayed better electrocatalytic activity and stability towards poisoning than PdRuSn/C and PtRu/C (E-TEK Inc.) nanocatalysts.

The Pd/C and PdSn/C were studied by Liu et al. [22] as catalysts for formic acid oxidation. PdSn/C has higher electrocatalytic activity for formic acid electro-oxidation than a comparative Pd/C catalyst and shows great potential as a less expensive electrocatalyst for formic acid electro-oxidation in direct formic acid fuel cells (DFAFCs).

Du et al. [23] studied a series of carbon-supported Pd–Sn binary alloyed catalysts for ethanol electro-oxidation in alkaline medium. Among various Pd–Sn catalysts, $Pd_{86}Sn_{14}$/C catalysts showed a great deal of enhanced current densities in cyclic voltammetric and chronoamperometric measurements, compared to commercial Pd/C (Johnson Matthey). The overall rate law of ethanol oxidation reaction, for both $Pd_{86}Sn_{14}$/C and commercial Pd/C, were also determined, clearly showing that $Pd_{86}Sn_{14}$/C was more favorable in high ethanol concentration and/or high pH environment.

Ramulifho et al. [24] studied the electrocatalytic oxidation of the ethylene glycol (EG) in alkaline medium using nano-scaled

palladium-based bimetallic catalysts (PdM, where M = Ni and Sn), supported on sulfonated multi-walled carbon nanotubes (SF-MWCNTs). The bimetallic mixture (i.e., SF-MWCNT–$PdSn_{mix}$ and SF-MWCNT–$PdNi_{mix}$) showed better electroactivity towards EG oxidation than SF-MWCNT–Pd. At SF-MWCNT–$PdSn_{mix}$ platform, EG oxidation occurred at lower onset and peak potentials, higher current density, and faster kinetics (lower impedance) than SF-MWCNT–$PdNi_{mix}$ platform. EG oxidation at SF-MWCNT–$PdNi_{mix}$ is more stable than SF-MWCNT–$PdSn_{mix}$. Indeed, Sn is a more favorable co-catalyst with Pd in EG electro-oxidation.

In a recent work, Geraldes et al. [25] prepared carbon-supported Pd, Au and bimetallic PdAu (Pd:Au 90:10, 50:50 and 30:70 atomic ratios) electrocatalysts using electron beam irradiation. Chronoamperometry (CA) experiments, at room temperature, revealed that PdAu/C electrocatalysts, with Pd:Au ratios of 90:10 and 50:50, presented superior activity toward ethanol electro-oxidation. *In situ* ATR-FTIR spectroscopy measurements have shown that the mechanism for ethanol electro-oxidation is dependent on catalyst composition, leading to different reaction products, such as acetaldehyde and acetate, depending on the number of electrons transferred. Experiments on a single ADEFC were conducted between 50 and 90 °C, and the best performance of 44 mW cm^{-2} in 2.0 mol L^{-1} ethanol was obtained at 85 °C for Pd:Au with Pd:Au atomic ratio 90:10 electrocatalyst.

Considering that PtSn/C electrocatalysts prepared by an electron beam irradiation method showed good activity for ethanol electro-oxidation in acid medium [13], PdSn/C electrocatalysts have been shown good activity for ethanol electro-oxidation in alkaline medium [20,21,23], the carbon supports influences the activity of the catalysts [12] and the results for PdSn electrocatalysts as anodes in alkaline DEFC conditions are scarce, in this work, Pd and PdSn with atomic ratio of 90:10 were supported on MWCNT and on Carbon Vulcan XC72 using an electron beam irradiation method. The obtained materials were characterized and tested for ethanol electro-oxidation in alkaline medium using electrochemical techniques. Pd/C, Pd/MWCNT, PdSn/C and Pd/MWCNT were also tested as anodes in an alkaline DEFC while Pd/C or Pd/MWCNT was used as cathodes.

2. Experimental

Multi wall carbon nanotubes (MWCNT), grown by the method of chemical vapor deposition (CVD), were provided by the Laboratory of Nanomaterials of the Department of Physics from Universidade Federal de Minas Gerais (UFMG). MWCNTs function was carried out in 50/50 (v/v) water/ethanol and was, then, dispersed in the solution using an ultrasonic bath. The resulting mixtures were submitted (at ambient conditions) under stirring to electron beam irradiation (Electron Accelerator's Dynamitron Job 188–IPEN/CNEN–SP), with a total applied dose of 288 kGy (dose rate 1.6 kGy s^{-1}, time 3 min). After electron beam irradiation, the mixtures were filtered and the solids (MWCNT) were washed with water and dried at 70 °C for 10 h.

Pd/C, Pd/MWCNT, PdSn/C and PdSn/MWCNT, with Pd:Sn atomic ratios 90:10 electrocatalysts (20 wt% metal loading), were prepared using $Pd(NO_3)_2.2H_2O$ (Fluka) and $SnCl_2$ (Fluka) as metal sources, dissolved in 50/50 (v/v) water/2-propanol. Carbon Vulcan® XC72R or MWCNT, used as a support, was, then, dispersed in the solution using an ultrasonic bath. The resulting mixtures were submitted (at ambient conditions) to stirring under electron beam irradiation (Electron Accelerator's Dynamitron Job 188–IPEN/CNEN–SP), with a total applied dose of 288 kGy (dose rate 1.6 kGy s^{-1}, time 3 min). After electron beam irradiation, the mixtures were filtered and the solids (Pd/C, PdSn/C, Pd/MWCNT and PdSn/MWCNT electrocatalysts) were washed with water and dried at 70 °C for 2 h, in agreement with a previous work [25].

Table 1
Nominal Pd:Sn atomic ratios, those obtained by EDX and crystallite sizes estimated by Debye–Scherrer's equation of PdSn/C and PdSn/MWCNT electrocatalysts, were prepared using electron beam irradiation.

Pd:Sn atomic ratio (nominal)	Pd:Sn atomic ratio (EDX)	Crystallite size (nm)
PdSn/C 90:10	91:09	3.7
PdSn/MWCNT 90:10	86:14	3.0

Pd:Sn atomic ratios were obtained by energy-dispersive X-ray analysis (EDX), using a Philips XL30 scanning electron microscope, with a 20 keV electron beam and equipped with an EDAX DX-4 microanalyzer.

X-ray diffraction (XRD) analyses were carried out with a Miniflex II, model Rigaku diffractometer, using a Cu Kα source (λ = 1.54056 Å). The diffractograms were recorded at 2θ in the range 20–90°, with step size of 0.05° and scan time of 2 s per step. The average crystallite size was estimated using the Debye-Scherer's equation [26].

Transmission electron microscopy (TEM) was carried out using a JEOL JEM-2100 electron microscope, operated at 200 kV. The particle distribution histogram was determined by measuring about 150 particles, from each micrograph.

Electrochemical studies were carried out using the thin porous coating technique [27]. A total of 20 mg of the electrocatalyst was added to a solution of 50 mL of water containing 3 drops of a 6% polytetrafluoroethylene (PTFE) suspension. The resulting mixture was treated in an ultrasound bath for 10 min, filtered and transferred to the cavity (0.30 mm deep and 0.36 cm^2 in area) of the working electrode. The reference electrode was Ag/AgCl (KCl 3 mol L^{-1}) homemade electrode, and the counter electrode was a Pt plate.

Electrochemical measurements were carried out using an AutoLab PGSTAT 30 potentiostat/galvanostat. Cyclic voltammetry was performed using 1.0 mol L^{-1} ethanol in 1.0 mol L^{-1} KOH, saturated with N_2. Chronoamperometry experiments were performed using 1.0 mol L^{-1} ethanol in 1.0 mol L^{-1} KOH at −0.40 V vs. Ag/AgCl, at room temperature.

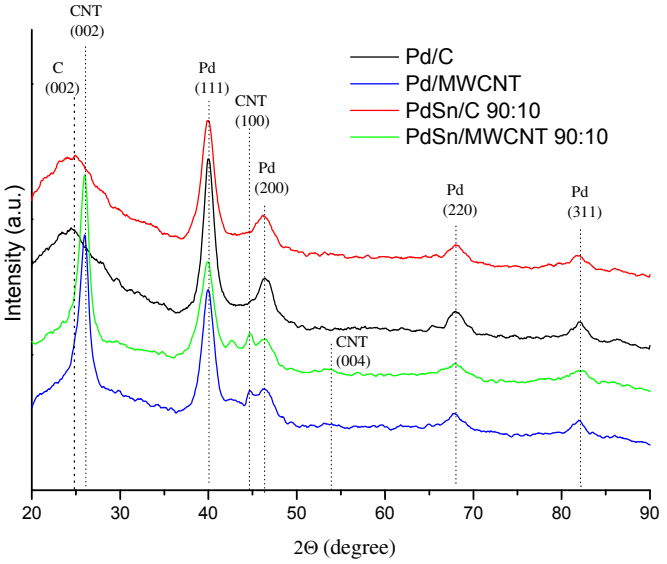

Fig. 1. X-ray diffractograms of Pd/C, Pd/MWCNT, PdSn/C (Pd:Sn atomic ratio 90:10) and PdSn/MWCNT (Pd:Sn atomic ratio 90:10) electrocatalysts prepared using electron beam irradiation.

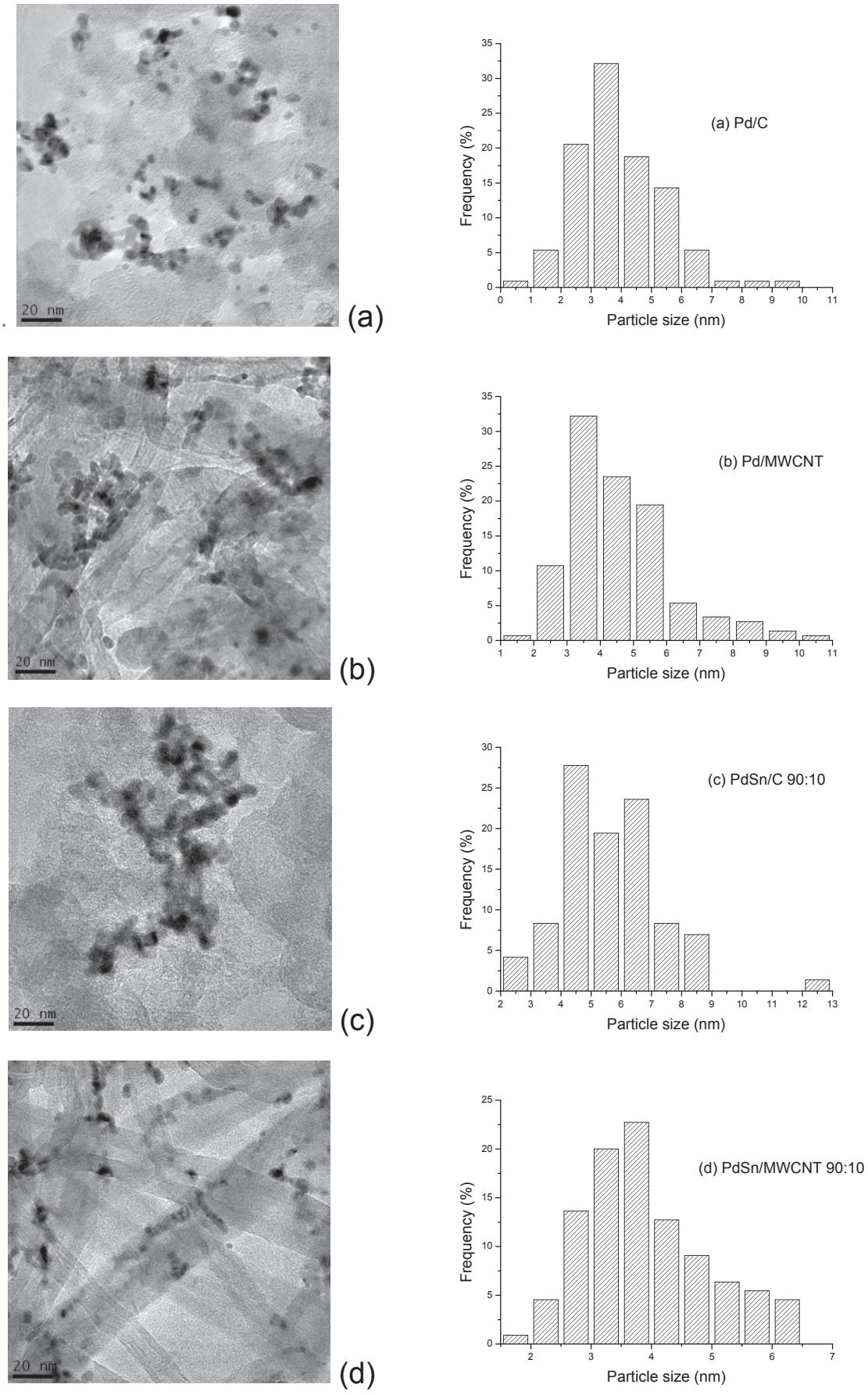

Fig. 2. TEM micrographs and particle size distribution histograms of (a) Pd/C, (b) Pd/MWCNT, (c) PdSn/C (90:10) and (d) PdSn/MWCNT (90:10) electrocatalysts.

In situ attenuated total reflectance Fourier transformed infrared spectroscopy (ATR-FTIR) measurements were carried out using a Varian® 660 IR spectrometer, equipped with an MCT detector cooled with liquid N_2, a MIRacle with a Diamond/ZnSe Crystal Plate (Pike®) ATR accessory and a special cell, as presented in the reference [17]. The same working electrode used in the electrochemical experiments was used in ATR-FTIR measurements. These experiments were performed at 25 °C in a 1.0 mol L^{-1} KOH solution containing 1.0 mol L^{-1} ethanol. The spectra were collected as ratio R:R_0, where R represents a spectrum at a given potential, and R_0 is the spectrum collected at −0.70 V. Positive and negative directional bands represent gains and losses of species at the sampling potential, respectively. The spectra were computed from 96 interferograms, averaged from 2500 to 850 cm^{-1}, with constant spectral resolution of 8 cm^{-1}. Initially, a reference spectrum, R_0, was measured at −0.70 V vs. Ag/AgCl (in this potential, the ethanol electro-oxidation has not yet begun and it is still in the hydrogen adsorption/desorption region); sample spectra were collected after applying successive potential steps from −0.85 to +0.20 V vs Ag/AgCl.

Membrane electrode assemblies (MEA) were prepared by hot pressing a Fumasep-FAA3-PEEK membrane (Fumasep FAA3 reinforced with PEEK and pre-treated in 1.0 mol L^{-1} KOH, for 24 h), between an anode of either Pd or PdSn, supported by C or MWCNT (prepared in this work) and a cathode of 20 wt% Pd/C or Pd/MWCNT, at 80 °C, for 2 min, under pressure of 45 kgf cm^{-2}. Both electrodes used 1.0 mg Pd cm^{-2} catalyst loading. The ink, containing 70 wt% catalysts + support and 30 wt% Nafion, was painted in carbon cloth. The MEA were placed between two bipolar plates and assembled in a single fuel cell with a 6 Nm torque wrench. The experiments were performed using a test bench from Electrocell Group that allows control over the fuel cell operating parameters (flow rates, humidification and temperature of the reactants and cell temperature), performing automatic data acquisition of polarization curves and power density curves, in real time. Liquid fuel alimentation made use of a Masterflex L/S Cole-Parmer peristaltic pump. The direct ethanol fuel cell performances were determined in a single cell with a geometric area of 5 cm^2. The temperature was set between 60 and 90 °C, for the fuel cell, and 85 °C for the oxygen humidifier. The 2.0 mol L^{-1} ethanol fuel, in 2.0 mol L^{-1} KOH, was delivered at 1.0 mL min^{-1}, and the oxygen flow was regulated at 500 mL min^{-1}. Polarization curves were obtained by using a CDE electronic load.

3. Results and discussion

The atomic ratios obtained by EDX for PdSn/C and PdSn/MWCNT electrocatalysts, prepared with Pd:Sn atomic ratios 90:10, are summarized in Table 1.

For all samples, Pd:Sn atomic ratios determined by EDX analysis was similar to the nominal ones, indicating that most of the metal ions contained in the mixtures were reduced to metal and chemically anchored to the supports (C and MWCNT).

The XRD diffractograms of Pd/C, Pd/MWCNT, PdSn/C and PdSn/MWCNT (Pd:Sn atomic ratios 90:10) electrocatalysts were displayed in Fig. 1.

The X-ray diffractograms displayed in Fig. 1 show a broad peak centered at about 2θ = 25° (Bragg angle) that was attributed to reflection plane (002) of the hexagonal structure of Carbon Vulcan XC-72R (C) and three sharp peaks at 2θ, about 26°, 44° and 54° that were attributed to reflections planes (002), (100) and (004), respectively, of the MWCNT support. The narrowing of the peaks associated with the MWCNT compared to Carbon was due to the greater MWCNT crystallinity. The four diffraction peaks related to the Pd are showed at 2θ, approximately, 40°, 46°, 68° and 82°, associated with the reflection planes (111), (200), (220) and (311), respectively, which are characteristic of the face-centered cubic (fcc) structure of Pd and Pd alloys [14,28–30]. It is observed, for PdSn catalysts, that the Pd (fcc) peaks were not shifted in relation to Pd catalysts, showing that PdSn alloys were not formed; moreover, diffraction peaks associated to metallic Sn and/or SnO_2 [31,32] were not observed. Our previous study [13], also, showed only the presence of Pt (fcc) phase in the X-ray diffractograms of PtSn/C electrocatalysts prepared by electron beam irradiation reduction; however, ^{119}Sn Mössbauer spectroscopy studies showed the presence of SnO_2 as an amorphous phase. The average crystallite size of Pd (fcc) phase was estimated based on the (220) peak width, at half height, according to the Debye–Scherer's equation. The (220) peak was chosen to avoid the interference from the diffraction peak of the carbon support. The estimated Pd (fcc) crystallite sizes of Pd/C, Pd/MWCNT, PdSn/C (Pd:Sn atomic ratio 90:10) and PdSn/MWCNT (Pd:Sn atomic ratio 90:10) electrocatalysts were 4.3, 4.3, 3.7 and 3.0 nm, respectively.

TEM micrographs of electrocatalysts studied show morphology, particle size and their distribution histograms in Fig. 2.

The micrographs of Pd/C and PdSn/C electrocatalysts showed higher amount of agglomerates. Such features reduce the surface area required for fuel adsorption, reducing the electrocatalysts activities. TEM micrographs, also, show that MWCNT-supported electrocatalysts (Pd/MWCNT and PdSn/MWCNT) present reduced particle sizes compared to carbon-supported electrocatalysts. Although these electrocatalysts do not form alloy, as shown in XRD analysis, however, they have greater surface area available for fuel adsorption and there is the possibility that the metals can provide synergism to facilitate oxidation of the fuel and its intermediates via bifunctional mechanism. The average particle size of Pd/C, Pd/MWCNT and PdSn/MWCNT electrocatalysts are between 3.0 and 4.0 nm, while for PdSn/C is between 4.0 and 5.0 nm.

CVs of electrocatalysts studied in 1.0 mol L^{-1} KOH are shown in Fig. 3.

The cyclic voltammograms display the behavior of Pd/C, Pd/MWCNT, PdSn/C and PdSn/MWCNT(Atomic ratios Pd:Sn = 90:10) electrodes under the influence of the potential sweep between −0.85 V and +0.2 V vs. Ag/AgCl. The voltammetric response of the four electrodes is a characteristic of Pd-supported electrodes, in basic medium, and represents the current

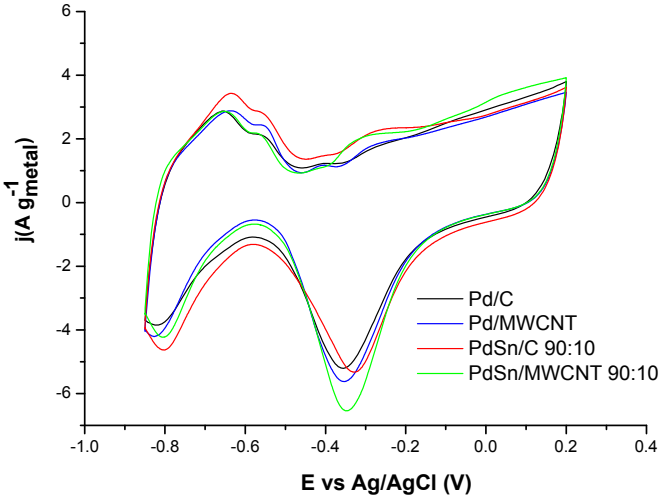

Fig. 3. Cyclic voltammograms of Pd/C, Pd/MWCNT and PdSn/C, Pd/MWCNT (Pd:Sn atomic ratios 90:10) electrocatalysts in 1.0 mol L^{-1} KOH, measured over a potential range from −0.85 to 0.20 V vs. Ag/AgCl, at scan rate of 10 mV s^{-1}.

generated by several electrochemical processes occurring during this sweep potential. On the anodic sweep is possible to observe three main electrodic processes: surface oxides reduction (from −0.8 V to −0.75 V vs. Ag/AgCl), adsorbed hydrogen oxidation (from −0.75 V to −0.55 V vs. Ag/AgCl) and oxide/hydrous oxides Pd formation (from −0.40 V to +0.20 V vs. Ag/AgCl). In the cathodic sweep, it is possible to observe the Pd oxides reduction (around −0.35 V vs. Ag/AgCl) and hydrogen adsorption (around −0.85 V vs. Ag/AgCl). Despite having similar voltammetric profiles, each voltammogram has small differences in important regions for ethanol adsorption and electro-oxidation. On the anodic sweep, the cyclic voltammograms corresponding to electrocatalysts presented two broad peaks centered in −0.65 V and −0.55 V vs. Ag/AgCl, attributed to hydrogen desorption (weakly bond and strongly bond, respectively) process on Pd surface, suggesting that electrocatalysts prepared with these characteristics have facility for hydrogen and ethanol adsorption. The shoulders between −0.30 V and +0.20 V vs. Ag/AgCl are associated with the formation of Pd oxide layer, in different oxidation states on Pd surface {Pd(0), Pd(I), Pd(II) and Pd(IV)}, according to observations by Hu et al. [33].

The electrochemical activity of an electrocatalyst, evaluated by cyclic voltammetry, may be normalized either by electrochemically active surface area (ECSA) or by mass of electrocatalyst, both options have their deficiencies. In an acidic environment with Pt electrocatalyst, it is common to normalize the charge deposited/electrochemical activity by Platinum ECSA available for hydrogen adsorption. Thus, supposing that the voltammetric area of the curve over the hydrogen desorption peak (in desorption/adsorption hydrogen region) is numerically equal to the charge of a monolayer of hydrogen deposited on the active electrocatalyst surface and assuming that the charge for monolayer adsorption/desorption of hydrogen on Pt is 210 μC cm^{-2}. It is possible to determine the active surface area available for the hydrogen adsorption on Pt, but, in alkaline environment, it is not reasonable to derive the Pd ECSA electrocatalyst from the hydrogen region, since Pd is known to efficiently absorb hydrogen, which can diffuse into the Pd bulk, to form Pd hydride rather than adsorbing onto the Pd surface [34,8]. Thus, in alkaline environment with Pd electrocatalyst, the ECSA is estimated using the area over the voltammetric curve in the palladium oxides reduction peak region. However, in this work, the CV responses were normalized per metal gram, since the work electrodes were rough electrodes prepared by the thin porous coating technique. Therefore, the electrode has many catalyst sites covered and, for this reason, the normalization by active surface area was not used. Furthermore, the actual performance of an electrocatalyst is better defined when using a language close to the commercial one, if purchasing electrocatalyst per gram, not by active area.

On cathodic sweep, it was also observed that the cyclic voltammograms, representing the MWCNT-supported electrocatalysts, showed more prominent peaks reduction of the different oxides formed during the anodic sweep (around −0.35 V vs. Ag/AgCl) and a smaller curve widening in the region −0.58Vvs. Ag/AgCl, suggesting the existence of (a) a smaller quantity of Pd/Sn oxides or (b) the consequence of the MWCNT support influence, making the electrode less resistive [35].

The voltammetric responses for ethanol electro-oxidation using Pd/C, Pd/MWCNT, PdSn/C (Pd:Sn atomic ratio 90:10) and PdSn/MWCNT (Pd:Sn atomic ratio 90:10) electrocatalysts are shown in Fig. 4.

In all CVs, the voltammetric responses (current values) were normalized per gram of metal, although the ethanol adsorption and dehydrogenation occurs, preferentially, in palladium sites, at room temperature [26]; it was observed that the hydrogen adsorption/desorption region, compared to previous CVs (Fig. 3), was significantly suppressed by the presence of ethanol. The Pd/MWCNT and PdSn/MWCNT cyclic voltammograms showed that the potential beginning of the ethanol electro-oxidation (onset potential) was smaller than the others (−0.69 V vs. Ag/AgCl); there was a higher current density towards ethanol electro-oxidation in alkaline medium in the whole potential range evaluated, confirming that MWNTC-supported electrocatalysts are more efficient than C-supported electrocatalysts. This occurs, probably, due to the smaller resistivity of electrodes and better particle distribution on the substrate, allowing a higher active surface area exposed, as shown in TEM analysis [12]. The Pd/C and PdSn/C CVs presented onset potential 0.05 V higher than others and lower electrocatalytic activity toward ethanol electro-oxidation over the entire potential range, including the region of interest of ADEFC (−0.45 V to −0.35 V vs Ag/AgCl). These results suggest that both the presence of the second metal and the chemical composition of support can improve the supported-electrocatalyst activity.

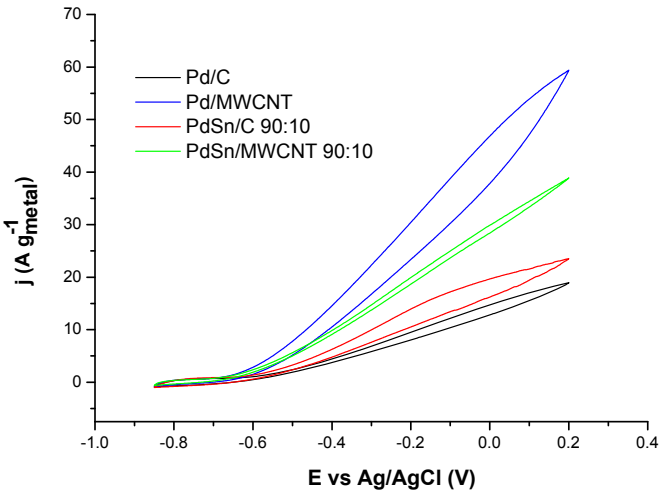

Fig. 4. Cyclic voltammograms of Pd/C, Pd/MWCNT, PdSn/C (Pd:Sn atomic ratio 90:10) and PdSn/MWCNT (Pd:Sn atomic ratio 90:10) electrocatalyst using 1.0 mol L^{-1} ethanol and 1.0 mol L^{-1} KOH, measured over potential range from −0.85 to +0.20 V vs. Ag/AgCl, at sweep rate of 10 mV s^{-1}.

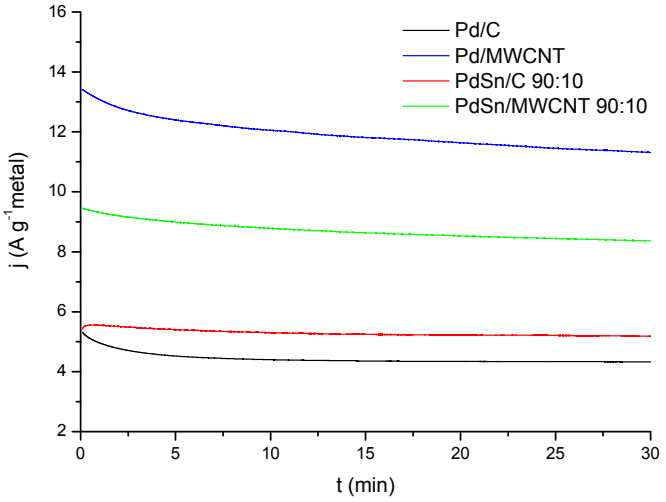

Fig. 5. Current-time curves at −0.40 V for Pd/C or MWCNT and PdSn/C or MWCNT (Pd:Sn atomic ratio of 90:10) electrocatalyst, using 1.0 mol L^{-1} ethanol in 1.0 mol L^{-1} KOH.

The chronoamperometry curves for ethanol oxidation using Pd/C, Pd/MWCNT, PdSn/C (Pd:Sn atomic ratio 90:10) and PdSn/MWCNT (Pd:Sn atomic ratio 90:10) electrocatalysts, obtained at room temperature, using 1.0 mol L^{-1} ethanol in 1.0 mol L^{-1} KOH, at a fixed potential of −0.40 V vs. Ag/AgCl for 30 min, are shown in Fig. 5.

The electrocatalysts prepared were tested for 30 min to evaluate the electrocatalysts activity, stability and tolerance to poisoning by intermediate species. In all experiments, the current density reaches a stable condition and the electrocatalyst stability can be evaluated. It is still worthwhile to note that Pd/MWCNT and PdSn/MWCNT 90:10 electrocatalysts have a higher electrocatalytic activity towards ethanol electro-oxidation, compared to others, although they showed a slight current decay, probably due to a greater fuel consumption from higher currents or due to the deactivation of their catalytic sites. The current values of the Pd/C and PdSn/C electrocatalysts remained smaller along the time.

The identification of products generated during ethanol electro-oxidation was carried out by *in situ* FTIR in the range of −0.70 to 0.20 V vs. Ag/AgCl using Pd and PdSn 90:10 electrocatalysts

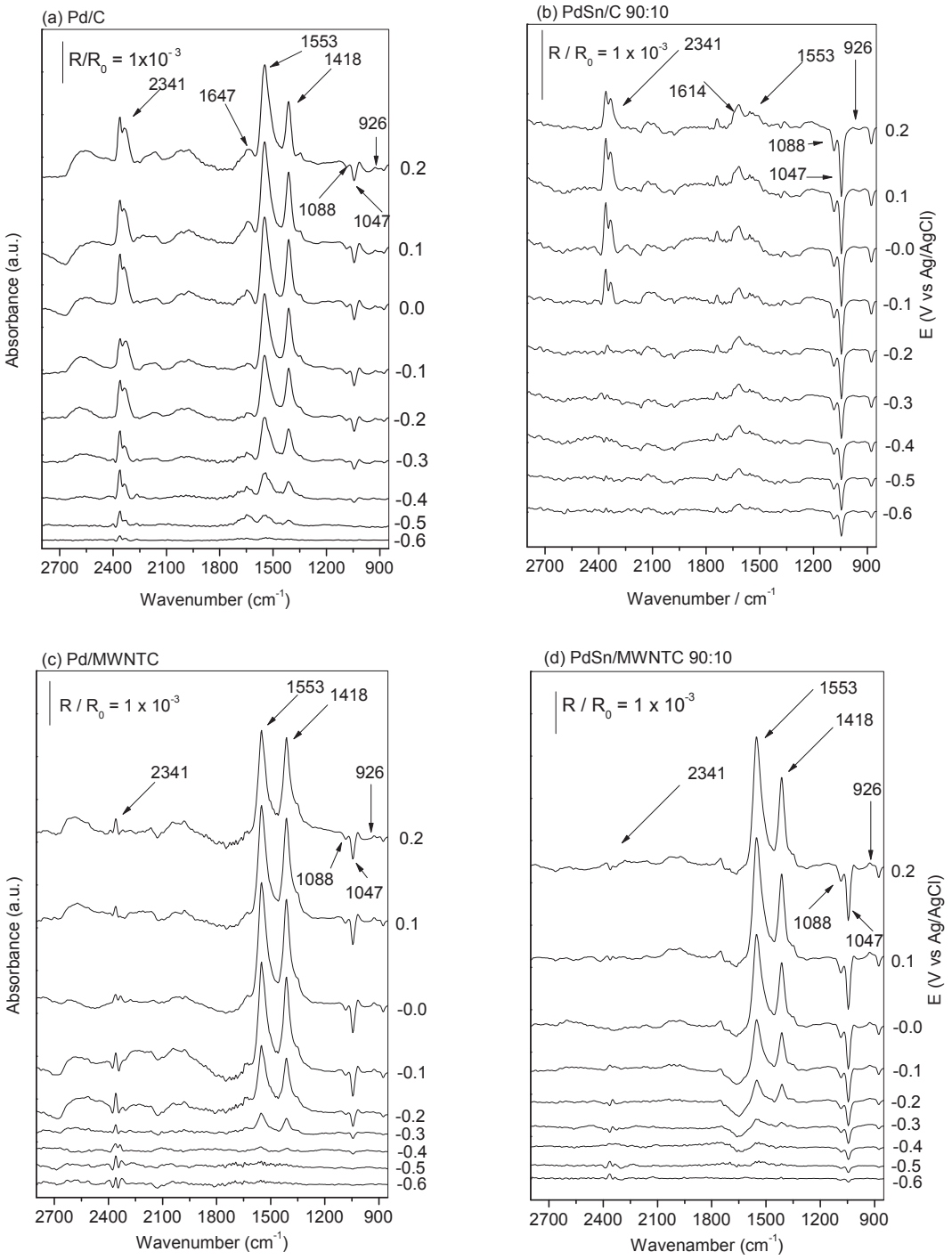

Fig. 6. *In situ* FTIR spectra of Pd and PdSn 90:10 electrocatalysts supported in C (a, b) or MWNTC (c, d) electrocatalysts, taken in the potential range −0.70 to 0.20 V vs. Ag/AgCl, using 1.0 mol L^{-1}ethanol in 1.0 mol L^{-1} KOH. Each spectrum corresponds to an increase of 0.1 V compared with the spectrum below it.

supported in C or MWNTC. FTIR spectra (Fig. 6) were recorded with 0.10 V increments, using 1.0 mol L^{-1} ethanol in 1.0 mol L^{-1} KOH aqueous solution, at room temperature.

The Pd/C, Pd/MWNTC and PdSn/MWNTC electrocatalysts spectra display two intense peaks at 1553 and 1418 cm^{-1}, originating from asymmetric and symmetric C–O bond vibrations that are characteristic of the presence of acetate ions. The PdSn/C electrocatalyst presents peak at 1553 cm^{-1} less intense. The small peak at 926 cm^{-1} is associated with acetaldehyde originating from stretching C–O–O bond vibrations [36,37]. The band at 2341 cm^{-1} was associated with CO_2 symmetric stretching vibrations and was observed with higher intensity in Pd/C and PdSn/C electrocatalysts. In Pd/MWNTC and PdSn/MWNTC electrocatalysts this band was less intense, suggesting the presence of small amount of CO_2. These spectra also show the presence of peaks at 1047 and 1088 cm^{-1} that are associated with ethanol consumption [39]. These bands are more pronounced for PdSn/C and PdSn/MWNTC electrocatalysts, indicating higher ethanol consumption.

The variations of acetate, acetaldehyde and CO_2 bands intensities with potential were analyzed individually to compare the Pd/C, Pd/MWNTC, PdSn/C 90:10 and PdSn/MWNTC 90:10 electrocatalysts and the results are shown in Fig. 7.

The generation level of acetate is similar for Pd/C, Pd/MWNTC and PdSn/MWNTC electrocatalysts over the entire potential range, but the presence of acetate beginning at different potentials for each electrocatalyst. For PdSn/C electrocatalyst the generation level of acetate is lower than the other ones. In the case of acetaldehyde, a higher generation level were observed for the electrocatalysts MWNTC-supported in the potential range between −0.30 and 0.00 V vs. Ag/AgCl. In the PdSn/C 90:10 electrocatalyst spectrum the acetaldehyde was not detected. The generation level of CO_2 was higher in PdSn/C electrocatalyst. These results suggest that ethanol electro-oxidation on Pd/C, Pd/MWNTC and PdSn/MWNTC electrocatalysts in alkaline medium occurs predominantly without C–C bond breaking, thus lowering the amounts of carbonate ion and CO_2 generated; therefore, acetate and acetaldehyde are the main products. The formation of acetate and acetaldehyde not diminish the importance of the electrocatalyst because for the CO_2 generation requires formation of CO, which poisons the catalyst and has slower reaction kinetics. Furthermore, studies have shown that the amount of CO_2 formed is minimal, and the most active electrocatalysts are less selective to CO_2 and preferentially generate acetate and acetaldehyde [37,38].

The variations of acetate, acetaldehyde and CO_2 band intensity with potential were in Fig. 8 for Pd/C, Pd/MWNTC, PdSn/C 90:10 and PdSn/MWNTC 90:10 electrocatalysts.

It is well known that electrochemical oxidation of ethanol in alkaline medium can occur by three different routes: [39]

$$CH_3CH_2OH + 2OH^- \rightarrow CH_3CHO + 2H_2O + 2e^- \quad (1)$$

$$CH_3CH_2OH + 4OH^- \rightarrow CH_3COOH + 3H_2O + 4e^- \quad (2)$$

$$CH_3CH_2OH + 12OH^- \rightarrow 2CO_2 + 9H_2O + 12e^- \quad (3)$$

The results in Fig. 8 suggest that the Pd/C, Pd/MWNTC and PdSn/MWNTC electrocatalysts perform preferentially the ethanol electro-oxidation along the route of 4 electrons (major formation of acetate – Eq. (2)) while the PdSn/C electrocatalysts seems to occur by 12 electrons route (major formation of CO_2 – Eq. (3)).

The single fuel cells performance in the temperature range 60–90 °C of Pd/C, PdSn/C(Pd:Sn atomic ratio = 90:10), Pd/MWCNT and Pd/MWCNT (Pd:Sn atomic ratios 90:10) electrocatalysts, fed with 1.0 mL.min^{-1}using 2.0 mol L^{-1} ethanol in 2.0 mol L^{-1} KOH, at room temperature, are shown in Fig. 9.

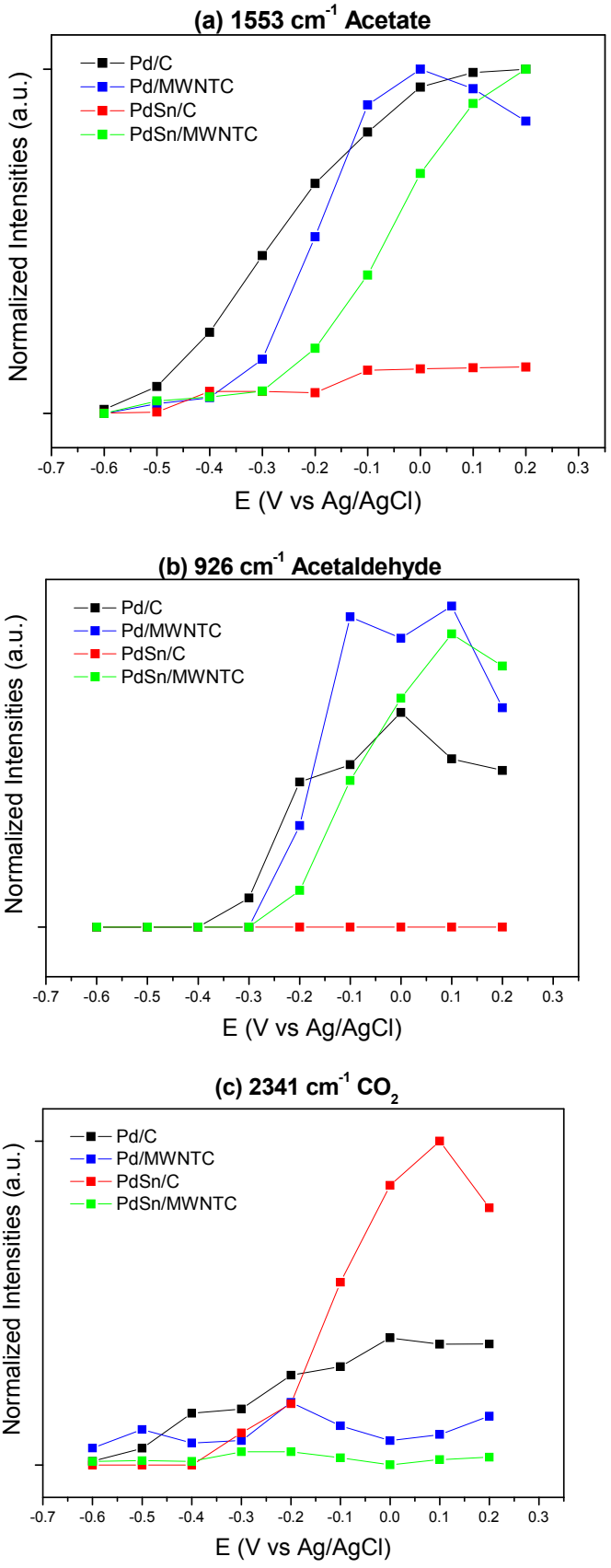

Fig. 7. Generation levels of acetate (a), acetaldehyde (b) and CO_2 (c) in the Pd/C, Pd/MWNTC, PdSn/C 90:10 and PdSn/MWNTC 90:10 electrocatalysts as a function of potential.

For all electrodes, the performance was significantly improved with the temperature increase, indicating that the ethanol electro-oxidation processes were thermally activated. The highest current and power densities were obtained at about 85 °C for PdSn/MWCNT (Pd:Sn atomic ratio 90:10) electrocatalyst. Above this temperature, independently of the support used, water management and membrane dryness and electrodes resistivity begin to degrade the performance of the electrodes, probably, owing to the increased cell resistance. At 90 °C, a decrease of the cell performance was observed. These results indicate that a better reactant diffusion and higher kinetics of the electrodes may be achieved at higher temperatures. No problems were detected with fuel diffusion in the electrodes since, in the polarization curves, a maximum current was reached without exponential decay associated to the mass transport limitations, i. e. the curves do not exhibit accentuated decay in the concentration over potential region. The increase of both OCV and power density, increasing the fuel cell temperature, also, suggests that the membrane used in MEA has

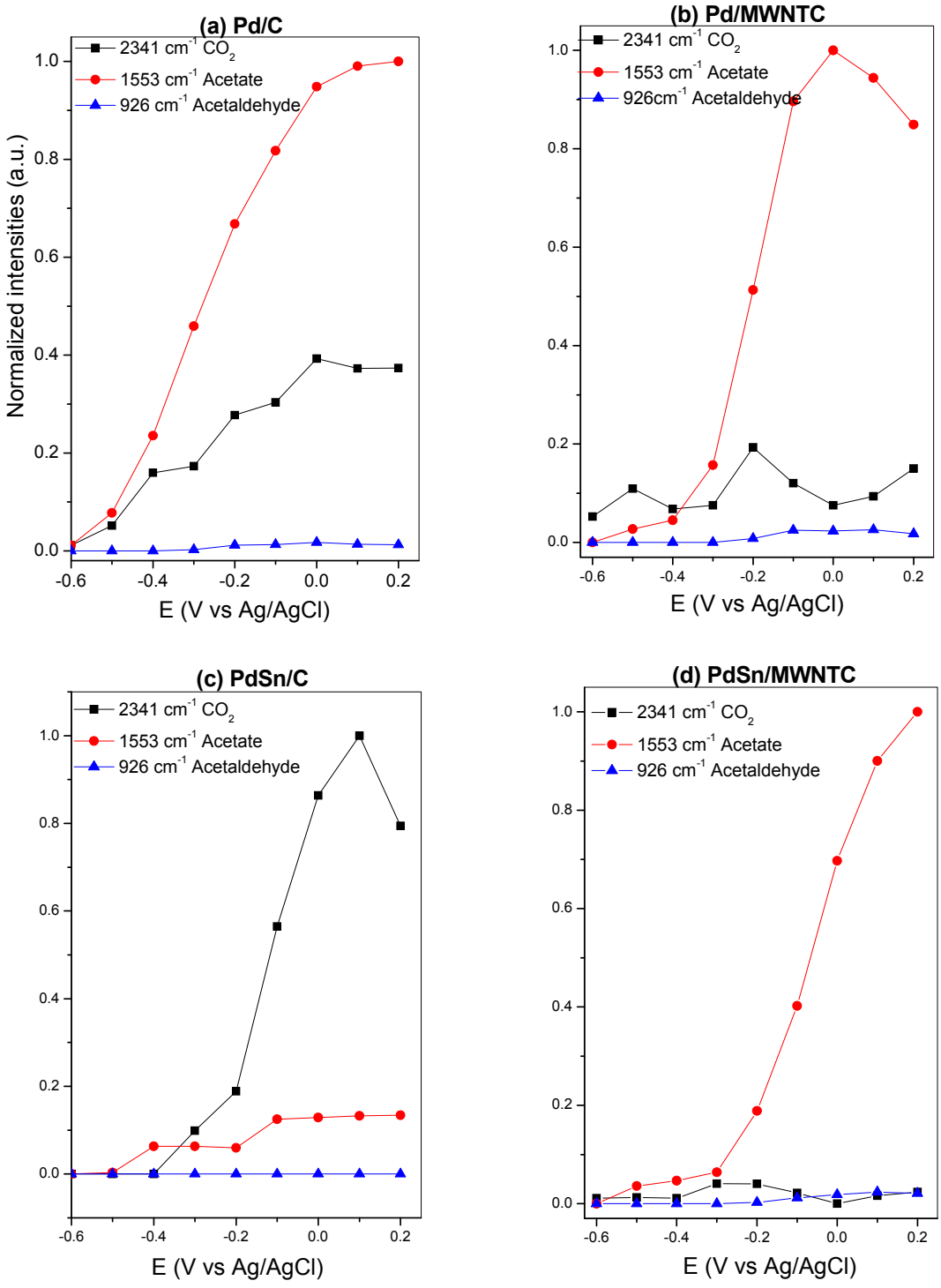

Fig. 8. Variations of acetate, acetaldehyde and CO_2 band intensity with potential for (a) Pd/C, (b) Pd/MWNTC, (c) PdSn/C 90:10 and (d) PdSn/MWNTC 90:10 electrocatalysts.

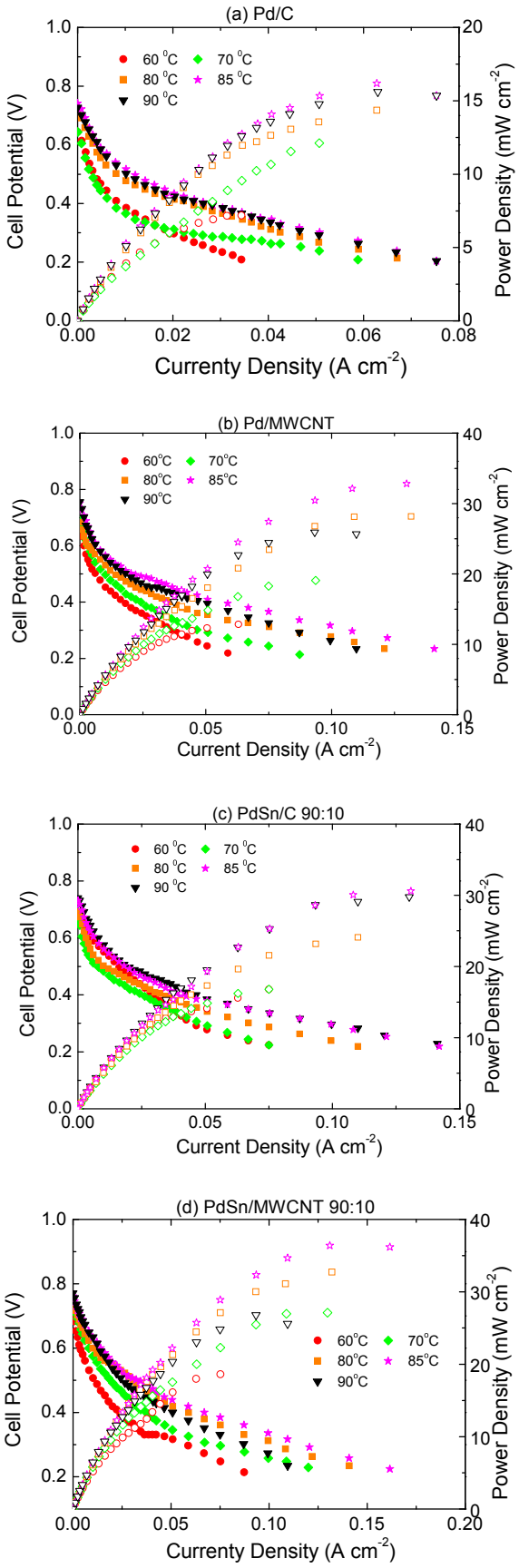

Fig. 9. Polarization and power density curves of a 5 cm^2 ADEFC, using a Fumasep-FAA-PEEK membrane, operating from 60 to 90 °C and using a (a) Pd/C, (b) Pd/MWCNT, (c) PdSn/C (Pd:Sn atomic ratio 90:10) and (d) PdSn/MWCNT (Pd:Sn atomic ratio 90:10) anodic electrocatalyst and a Pd/C or MWCNT cathodic electrocatalyst fed with 2.0 mol L^{-1} ethanol in 2.0 mol L^{-1} KOH solution; the anodic and cathodic catalyst loading levels were both 1 mg Pd cm^{-2} and oxygen humidifier, at a temperature of 85 °C.

low permeability to ethanol, since an increase in the cell operating temperature favors the ions mobility in the membrane, raising the fuel permeability toward the cathode. This fact would promote the occurrence of parallel reactions between the fuel and OH^- species, present in the cathode, creating a potential mix and reducing the cell overall potential. Nevertheless, this phenomenon was not observed in the graph [40].

Evaluating the support contribution, it was noticed that the maximum power density generated by the Pd/MWCNT electrocatalyst (33 mW cm^{-2}) was higher than that generated by the Pd/C electrocatalyst (16 mW cm^{-2}); this fact was attributed to the smaller size of the particles size, to a better distribution of metals on the MWCNT (Fig. 2) and to a higher support conductivity.

Nikolic et al. [34] have investigated the activity of tungsten carbide-supported Pd, tungsten carbide-supported Pt and Vulcan XC-72-supported Pd as anode catalysts for PEM fuel cells. The results presented show that all prepared catalysts are more active for hydrogen oxidation reaction than commercial platinum catalysts (Alpha Aesar). This fact was attributed to higher conductivity of tungsten carbide compared to that of VulcanXC-72.

Awasthi et al. [35] have prepared Graphene-supported Pd and Graphene-supported PdSn nanocomposites (Pd/GNS and PdSn/GNS), by microwave assisted polyol reduction method, and investigated their electrocatalytic activities toward the methanol electro-oxidation reaction. Their study showed that electrocatalytic performance of the Pd/GNS electrodes was observed to be the best option, with 20 wt% Pd loading; a higher or lower loading than 20 wt% Pd produces an electrode with, relatively, low catalytic activity. The apparent catalytic activity of this active electrode at E = −0.10 V was found to improve by 79% and CO poisoning tolerance by 40%, with introduction of 2 wt% Sn. The CO-poisoning tolerance efficiency of the active electrode (20%Pd/GNS) improved nearly 32% and 40% with 1 and 2 wt% Sn addition, respectively. Among the electrodes investigated, the 18%Pd–2%Sn/GNS exhibited the greatest electrocatalytic activity toward methanol electro-oxidation, in alkaline solution.

The maximum power density obtained by PdSn/MWCNT electrocatalyst (36 mW cm^{-2}) is higher than that obtained by PdSn/C electrocatalyst (30 mW cm^{-2}). The PdSn/MWCNT electrocatalyst shows higher power density throughout the potential examined. At the same conditions, ethanol electro-oxidation by Pd/MWCNT electrocatalyst produces around the double of power density generated by Pd/C, whereas the PdSn/MWCNT electrocatalyst only generates 20% more than PdSn/C electrocatalyst. These data suggest that both co-catalysts (Sn) and the support are important to catalytic activity and that, to a higher current density, a larger amount of Pd sites is necessary, once the increase in current was less significant (20%), probably due to (a) the presence of SnO_2, which increases the amount of oxides and reduces the available amount of Pd active sites and (b) due to a better distribution of nanoparticles in MWCNT. The single-cell tests showed that the addition of up to 10 at% of Sn, to Pd enhances the activity of PdSn electrocatalyst, independently from the support used.

The main results obtained on the single ADEFC experiments are summarized in Table 2.

The values in Table 2 revealed two principal observations: (i) in all temperature ranges, the power densities were higher when MWCNT-support was used; (ii) the highest power densities

Table 2
Values of maximum power density achieved in the temperature range 60–90 °C of Pd/C, PdSn/C (Pd:Sn atomic ratio = 90:10), Pd/MWCNT and Pd/MWCNT (Pd:Sn atomic ratio = 90:10) electrocatalysts, fed with 1.0 mL min^{-1} using 2.0 mol L^{-1} ethanol in 2.0 mol L^{-1} KOH, and oxygen flow of 500 mL min^{-1} (both at atmospheric pressure).

Temperature/°C	P_{max}/mW cm^{-2}			
	Pd/C	Pd/MWCNT	PdSn/C	PdSn/MWCNT
60	7.0	13	17	18
70	12	19	17	27
80	14	28	24	33
85	16	33	30	36
90	15	26	29	27

generated were at 85 °C, what it was, also, noticed previously by Geraldes et al. [25]. The highest power densities were 16, 33, 30 e 36 mW cm^{-2}, obtained with Pd/C, Pd/MWCNT, PdSn/C (Pd:Sn atomic ratio 90:10) and PdSn/MWCNT (Pd:Sn atomic ratio 90:10) MEAs, respectively. The literature [39] showed many results for alkaline DEFC, however, the comparison of our results with these studies is very difficult due the different materials (anionic membranes and catalysts) and conditions used (quantity of catalysts on anodes and cathodes, temperature, etc.), but the values described for power densities were in the range of 10–160 mW cm^{-2}.

4. Conclusions

The electron beam irradiation reduction method has showed to be an efficient method for the production of Pd/C, PdSn/C, Pd/MWCNT and PdSn/MWCNT electrocatalysts, for ethanol electro-oxidation in alkaline medium. Pd/MWCNT and PdSn/MWCNT electrocatalysts, in addition to having higher conductivity, also showed smaller particle sizes and better distribution on the support. At room temperature, electrochemical experiments (CV and CA) showed that MWCNT-supported Pd based electrocatalysts generated larger currents towards ethanol electro-oxidation than C-supported Pd based electrocatalysts. The *in situ* ATR-FTIR experiments identified acetate, CO_2 and acetaldehyde as the major products of ethanol electro-oxidation. In single fuel cell experiments, the best results were obtained at 85 °C and, again, the electrocatalysts prepared using MWCNT, as support, showed superior performance compared to that of materials C-supported. The best activity of MWCNT-supported electrocatalysts was attributed to their higher conductivity, smaller nanoparticles size and better distribution on the support. The promoting effect of tin has been explained by a bi-functional mechanism, in which Sn adsorbs and increases the concentration of OH^- species in proximity to Pd, favoring the ethanol/intermediary electro-oxidation adsorbed to the Pd surface.

Acknowledgments

The authors wish to thank FAPESP (2013/01557-0), CNPq (162669/2013-5, 406612/2013-7–474913/2012-0), INCT (573.783/2008-0) and CTR and CCTM from IPEN/CNEN-SP for electron beam irradiations and TEM measurements.

References

[1] F. Barbir, PEM Fuel Cells, Academic Press, Theobald's Road, London, 2013.
[2] M. Carmo, G. Doubek, R.C. Sekol, M. Linardi, A.D. Taylor, J. Power Sources 230 (2013) 169–175.
[3] A. Brouzgou, S.Q. Song, P. Tsiakaras, Appl. Catal. B: Environ. 1 27 (2012) 371–388.
[4] S.Y. Shen, T.S. Zhao, J.B. Xu, Y.S. Li, J. Power Sources 195 (2010) 1001–1006.
[5] A.O. Neto, R.R. Dias, M.M. Tusi, M. Linardi, E.V. Spinacé, J. Power Sources 166 (2007) 87–91.
[6] H. Liu, C. Song, L. Zhang, J. Zhang, H. Wang, D.P. Wilkinson, J. Power Sources 155 (2006) 95–110.
[7] A. Brouzgou, A. Podias, P. Tsiakaras, J. Appl. Electrochem. 43 (2013) 119–136.
[8] L.V. Kumar, S.A. Ntim, O.S. Khow, C. Janardhana, V. Lakshminarayanan, S. Mitra, Electrochim. Acta 83 (2012) 40–46.
[9] W.J. Zhou, W.Z. Li, S.Q. Song, Z.H. Zhou, L.H. Jiang, G.Q. Sun, Q. Xin, K. Poulianitis, S. Kontou, P. Tsiakaras, J. Power Sources 131 (2004) 217–223.
[10] S. Rousseau, C. Coutanceau, C. Lamy, J.M. Léger, J. Power Sources 158 (2006) 18–24.
[11] E. Antolini, J. Power Sources 170 (2007) 1–12.
[12] C. Bianchini, P.K. Shen, Chem. Rev. 109 (2009) 4183–4206.
[13] D.F. Silva, A.N. Geraldes, A.O. Neto, E.S. Pino, M. Linardi, E.V. Spinacé, W.A.A. Macedo, J.D. Ardisson, Mater. Sci. Eng. B 175 (2010) 261–265.
[14] D.F. Silva, A.O. Neto, E.S. Pino, M. Linardi, E.V. Spinacé, J. Power Sources 170 (2007) 303–307.
[15] D.F. Silva, A.O. Neto, E.S. Pino, M. Brandalise, M. Linardi, E.V. Spinacé, Mater. Res. 10 (2007) 367–370.
[16] D.F. Silva, A.N. Geraldes, E.Z. Cardoso, M.M. Tusi, M. Linardi, E.V. Spinacé, A.O. Neto, Int. J. Electrochem. Sci. 6 (2011) 3594–3606.
[17] J.C.M. Silva, L.S. Parreira, R.F.B. De Souza, M.L. Calegaro, E.V. Spinacé, A.O. Neto, M.C. Santos, Appl. Catal. B: Environ. 110 (2011) 141–147.
[18] R.F.B. Souza, J.C.M. Silva, F.C. Simões, M.L. Calegaro, A.O. Neto, M.C. Santos, Int. J. Electrochem. Sci. 7 (2012) 5356–5366.
[19] L. Jiang, A. Hsu, D. Chu, R. Chen, Int. J. Hydrogen Energy 35 (2010) 365–372.
[20] Q. He, W. Chen, S. Mukerjee, S. Chen, F. Laufek, J. Power Sources 187 (2009) 298–304.
[21] R.M. Modibedi, T. Masombuka, M.K. Mathe, Int. J. Hydrogen Energy 36 (2011) 4664–4672.
[22] Z. Liu, X. Zhang, Electrochem. Commun. 11 (2009) 1667–1670.
[23] W. Du, K.E. Mackenzie, D.F. Milano, N.A. Deskins, D. Su, X. Teng, ACS Catal. 2 (2012) 287–297.
[24] T. Ramulifho, K.I. Ozoemena, R.M. Modibedi, C.J. Jafta, M.K. Mathe, J. Electroanal. Chem. 692 (2013) 26–30.
[25] A.N. Geraldes, D.F. Silva, E.S. Pino, J.C.M. Silva, R.F.B. Souza, P. Hammer, E.V. Spinacé, A.O. Neto, M. Linardi, M.C. Santos, Electrochim. Acta 111 (2013) 455–465.
[26] V. Radmilovic, H.A. Gasteiger, P.N. Ross, J. Catal. 154 (1995) 98–106.
[27] A.O. Neto, M.J. Giz, J. Perez, E.A. Ticianelli, E.R. Gonzalez, J. Electrochem. Soc. 149 (2002) A272–A279.
[28] J. Belloni, M. Mostafavi, H. Remita, J.L. Marignier, M.O. Delcourt, New J. Chem. 22 (1998) 1239–1255.
[29] V. Bambagioni, C. Bianchini, A. Marchionni, J. Fillipi, F. Vizza, J. Teddy, P. Serp, M. Zhiani, J. Power Sources 190 (2009) 241–251.
[30] S.L. Medway, C.A. Lucas, A. Kowal, R.J. Nichols, D. Johnson, J. Electroanal. Chem. 587 (2006) 172–181.
[31] E.V. Spinacé, M. Linardi, A.O. Neto, Electrochem. Commun. 7 (2005) 365–369.
[32] W.S. Cardoso, M.S.P. Francisco, A.M.S. Lucho, Y. Gushikem, Solid State Ionics 167 (2004) 165–173.
[33] C.C. Hu, T.S. Wen, Electrochim. Acta 40 (1995) 495–503.
[34] V.M. Nikolic, D.L. Zugic, I.M. Perovic, A.B. Saponjic, B.M. Babic, I.A. Pasti, M.P.M. Kaninski, Int. J. Hydrog. Energy 38 (2013) 11340–11345.
[35] R. Awasthi, R.N. Singh, Int. J. Hydrog. Energy 37 (2012) 2103–2110.
[36] T. Yajima, N. Wakabayashi, H. Uchida, M. Watanabe, Chem. Commun. 7 (2003) 828–829.
[37] X. Fang, L. Wang, P.K. Shen, G. Cui, C. Bianchini, J. Power Sources 195 (2010) 1375–1378.
[38] M.M.O. Thotiyl, T.R. Kumar, S. Sampath, J. Phys. Chem. C 114 (2010) 17934–17941.
[39] E.H. Yu, U. Krewer, K. Scott, Energies 3 (2010) 1499–1528.
[40] Q.H. Zeng, Q.L. Liu, I. Broadwell, A.M. Zhu, Y. Xiong, X.P. Tu, J. Membr. Sci. 349 (2010) 237–243.